Supporting Information for

The tunable electronic structure and excellent catalytic properties of transition metal doped BeN_4 monolayer

*Wen-Hui Zhao[1], Dong-Yin Sun[1], Zi-Qiang Deng[1], Shi-Yao Liu[1], Lie-Mao Cao[1], Xiao-Hui Deng[1], Wen-Jin Yin[2], Zhen-Kun Tang[1]**

[1] *Key Laboratory of Micro-nano Energy Materials and Application Technologies, University of Hunan Province & College of Physics and Electronics Engineering, Hengyang Normal University, Hengyang 421002, China*

[2] *School of Physics and Electronic Science, Hunan University of Science and Technology, Xiangtan 411201, China*

**Email: zktang@hynu.edu.cn.*

The calculation method and corresponding formula for overpotential are shown as follows:

1. Nørskov's theoretical model

Following Nørskov's four step Proton-Coupled Electron Transfer (PCET) protocol, OER is a complex four electrons reaction pathway and the dissociation and adsorption of various oxygen intermediates, as following:

$$* + H_2O \rightarrow *OH + H^+ + e^- . \tag{1}$$

$$*OH \rightarrow *O + H^+ + e^- \tag{2}$$

$$*O + H_2O(l) \rightarrow *OOH + H^+ + e^- \tag{3}$$

$$*OOH \rightarrow * + O_2(g) + H^+ + e^- \tag{4}$$

Where * represents the transition metal (TM) active site on the surface of TM@BeN_4, *OH, *O, and *OOH was indicated as adsorbed oxygen intermediates. (l) and (g) represent liquid and gas phases respectively. The zero point energy (ZPE) and entropy (S) was included into the free energies calculations. The values of ΔZPE and ΔS were calculated from the vibrational frequencies of adsorbates on the catalyst surface at room temperature (T = 298.15 K), which respectively represent the change in zero-point energy and entropy. The change of Gibbs free energies defined as:

$$\Delta G = \Delta E + \Delta ZPE - T\Delta S \tag{5}$$

The OER catalytic activity can be evaluated by the magnitude of the potential-determining step under ideal conditions with U = 0 and standard hydrogen electrode (SHE), defines as overpotential (η_{OER}):

$$\eta_{OER} = max\,(\Delta G1, \Delta G2, \Delta G3, \Delta G4)/e - 1.23 \tag{6}$$

Generally, the lower η_{OER} is, the better OER catalytic activity would be.

2. Formation energy (E_{form})、 binding energy (E_{bind})、 cluster energy ($E_{cluster}$) and dissolution potential (U_{diss})

The calculation methods for formation energy (E_{form}) and binding energy (E_{bind}) are provided by Equation (7) and Equation (8) respectively, with detailed explanations of the variables in the equations as followed:

$$E_{form} = E_{dope} - (E_p - \mu_{Be} + \mu_{TM}) \tag{7}$$

$$E_{bind} = E_{dope} - E_{def} - E_{single} \tag{8}$$

Here, Ep and Edope represent the total energy of the pristine and TM doped BeN_4 monolayers, respectively. μ_{Be} and μ_{TM} are the chemical potentials of Be and the doped transition metals (Fe, Co, Ni, Ru, Rh, Pd, Ir, Pt), respectively. The E_{single} represents the energy of a single doped TM atom.

Table S1
Formation energy (E_{form}) and Binding energy (E_{bind}) of TM atoms doped in the BeN_4 Monolayer

TM	Fe	Co	Ni	Ru	Rh	Pd	Ir	Pt
E_{form} (eV)	1.74	1.38	1.88	3.79	2.72	3.32	3.17	3.17
E_{bind} (eV)	-9.47	-9.05	-7.17	-8.91	-8.76	-6.10	-9.61	-7.06

The calculation methods for cluster energy ($E_{cluster}$) and dissolution potential (U_{diss}) are provided by Equation (10) and Equation (11) as followed

$$E_{coh} = E_{TM-bulk}/n - E_{single} \tag{9}$$

$$E_{cluster} = E_{bind} - E_{coh} \tag{10}$$

$$U_{diss} = U^{\circ}_{diss} - E_{cluster}/Ne \tag{11}$$

Among these, E_{coh}, $E_{TM\text{-}bulk}$, E_{single}, $E_{cluster}$, and E_{bind} represent the cohesive energy of TM atoms, the total energy of TM bulk, the energy of a single TM atom, the cluster energy of TM@BeN_4, and the binding energy of TM@BeN_4, respectively. U°_{diss} represents the standard electrode potential of TM atoms. The quantity of TM in the bulk structure is denoted as n, and the number of electrons transferred during this process is denoted as Ne, the result is shown in Fig. S3. The calculated dissolution potentials of Fe, Co, Ni, Ru, Rh, Pd, Ir, and Pt in TM@NiN_2 structures are 0.57 V, 0.92 V, 0.68 V, 0.45 V, 1.12 V, 1.17 V, 1.36 V, and 1.48 V, respectively. While, the corresponding cluster energies of Fe, Co, Ni, Ru, Rh, Pd, Ir, and Pt are -2.03 eV, -2.39 eV, -1.89 eV, 0.02 eV, -1.05 eV, -0.45 eV, -0.60 eV, and -0.60 eV, respectively. The cluster energy ($E_{cluster}$) and dissolution potential (U_{diss}) of metal clusters in TM@BeN_4 structures were shown in Fig. S10. Notably, only Ru exhibits a positive cluster energy, suggesting the possibility of Ru cluster formation in Ru@BeN_4, which could impact the effective active sites and catalyst performance of SACs. Fortunately, the remaining TM@BeN_4 structures have the negative cluster energies and positive dissolution potentials, indicate that most of the considered TM@BeN_4 structures are thermodynamically and electrochemically stable under acidic conditions.

3. Support Figures

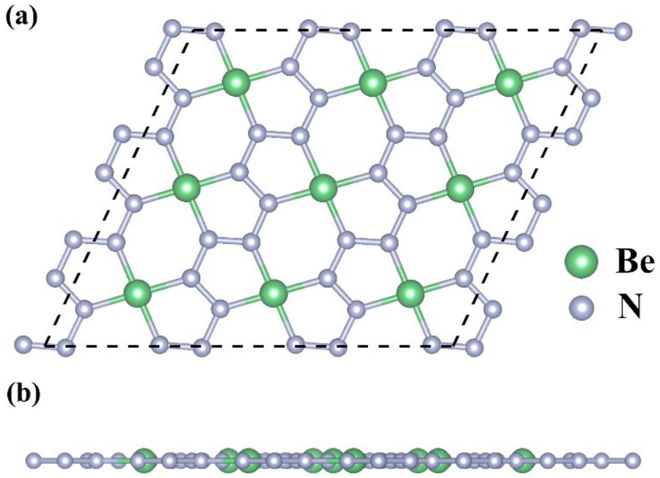

Fig. S1 *(a) Top view and (b) Side view of the* BeN_4 *monolayer structure. The green and gray spheres represent Be and N atoms, respectively.*

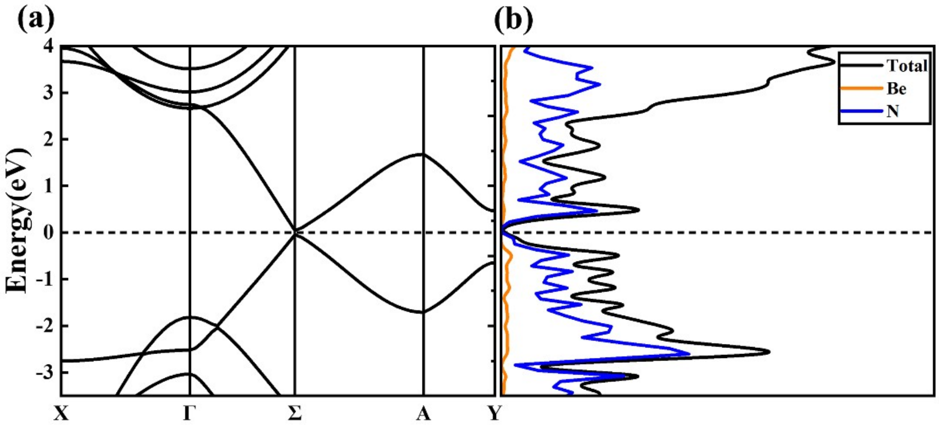

Fig. S2 *(a) Band structure and (b) density of states of the* BeN_4 *monolayer.*

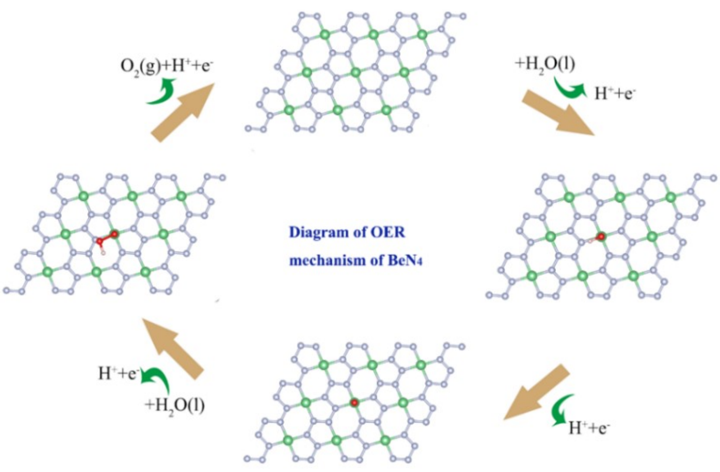

Fig. S3 *Schematic diagram of the OER process on pristine* BeN_4

In the overpotential step diagram, we present the results under three different potentials. The black line represents the initial state, the red line represents the equilibrium potential, and the blue curve represents the applied potential required to drive the reaction. This applied potential overcomes four energy barriers, causing the reaction to proceed, with the curve exhibiting a downward and relatively flat trend. The applied potential is the sum of the theoretical equilibrium potential and the overpotential. A lower applied potential indicates a more efficient catalyst.

The overpotential (η) was then obtained by subtracting the equilibrium potential from the applied potential ($E_{applied}$) needed to drive the reaction:

$$\eta = E_{applied} - E_{eq} \tag{12}$$

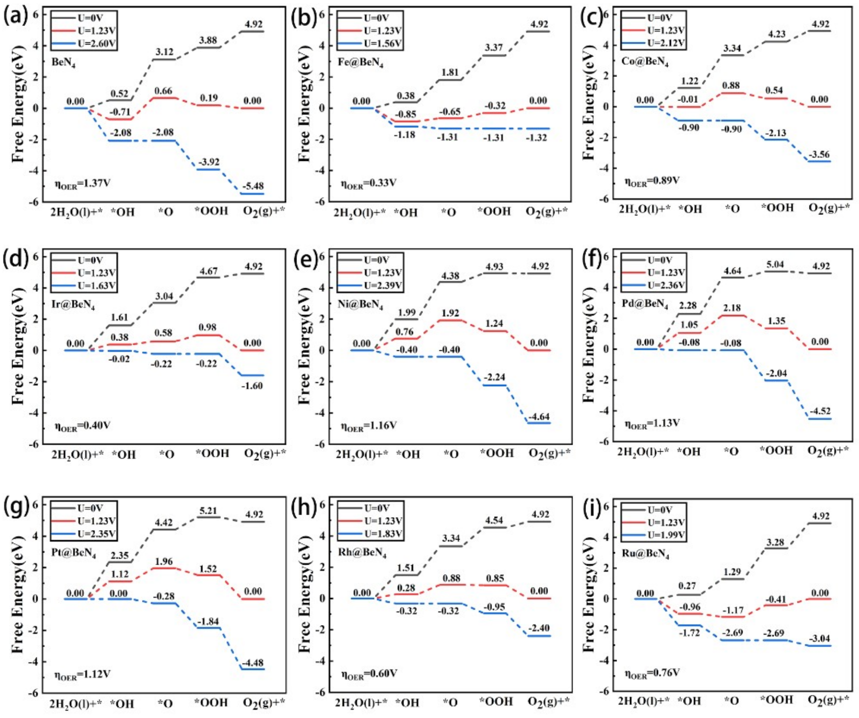

Fig. S4 *(a-i) Gibbs free energy step diagrams for OER at pH=0 of* BeN_4 *and TM@*BeN_4 *(TM = Fe,* *Ir, Ru, Co, Rh, Ni, Pd, Pt), the black, red, and blue lines represent the zero potential, the equilibrium potential, and the applied potential, respectively.*

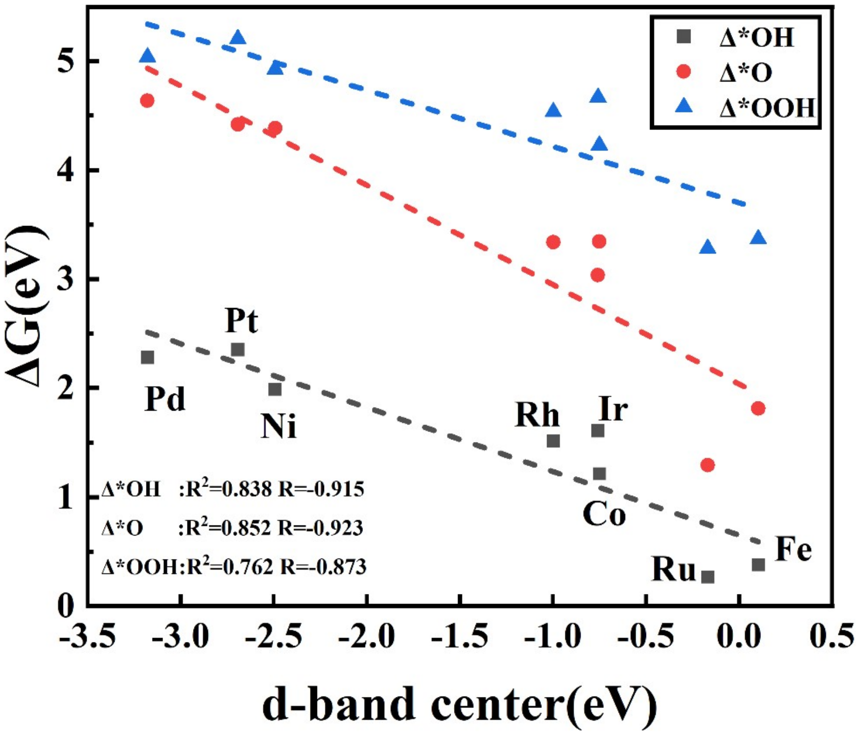

Figure S5 *Relationship between the Gibbs free energy of the three intermediates and the d-band center (ε_d). The black, red, and blue dashed lines are the fitted linear relationships between the Gibbs free energy of ε_d for *OH, *O, and *OOH, respectively. R^2 and R represent the coefficient of determination and correlation coefficient between the Gibbs free energy and the d-band center's respectively.*

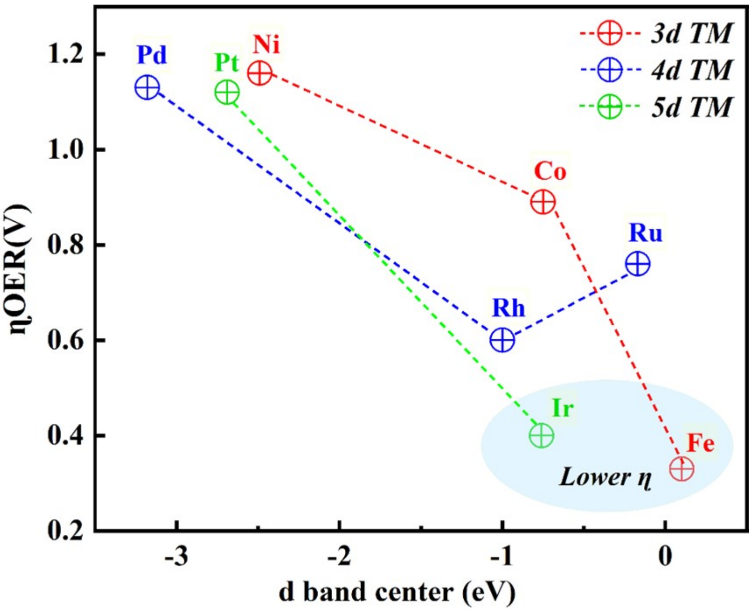

Figure S6 *The d band center against the OER overpotential for TM@ BeN_4 monolayers.*

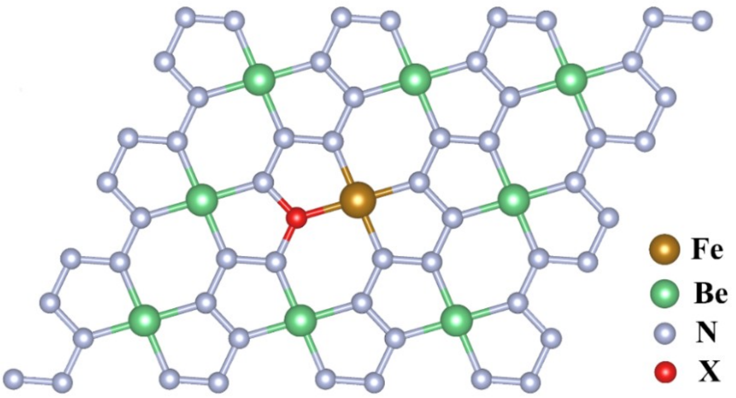

Fig. S7 *X-Fe@BeN$_4$ monolayer structure. The green, yellow, gray and red spheres represent Be, Fe, N and X (O, Be, C, P, S) atoms, respectively.*

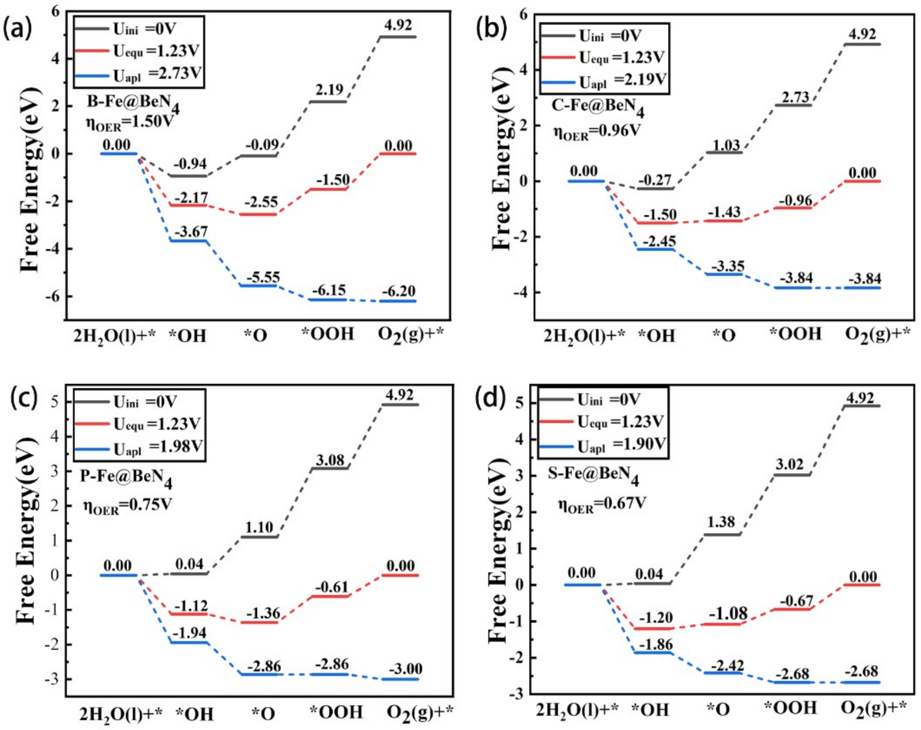

Fig. S8 *(a-d) Gibbs free energy step diagrams for OER at pH=0 of X-Fe@BeN$_4$ (X=B,C,P,S). The black, red, and blue lines represent the zero potential, the equilibrium potential, and the applied potential, respectively.*

We investigated the thermal stability of Fe@BeN$_4$ through ab-initio molecular dynamics (AIMD) simulations conducted in a canonical ensemble (NVT) using a Nose–Hoover thermostat with a time step of 1 fs. After 6 ps AIMD simulation at 300 K, the Fe@BeN$_4$ monolayer maintained its structural integrity, indicating strong thermal stability at room temperature."

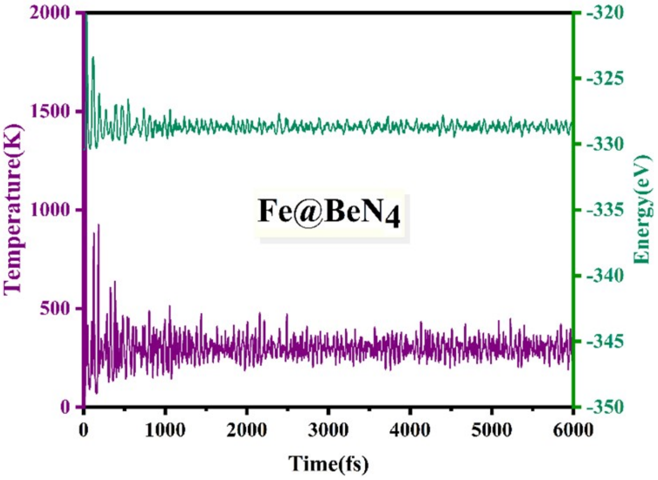

Fig. S9 *Energy and temperature variation with AIMD time for Fe@BeN$_4$ at 300 K.*

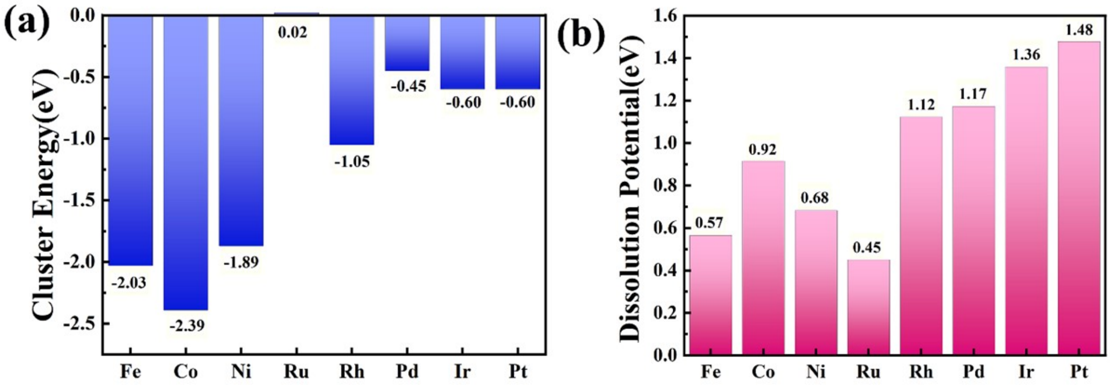

Fig. S10 *Cluster energy and dissolution points of TM@BeN$_4$.*

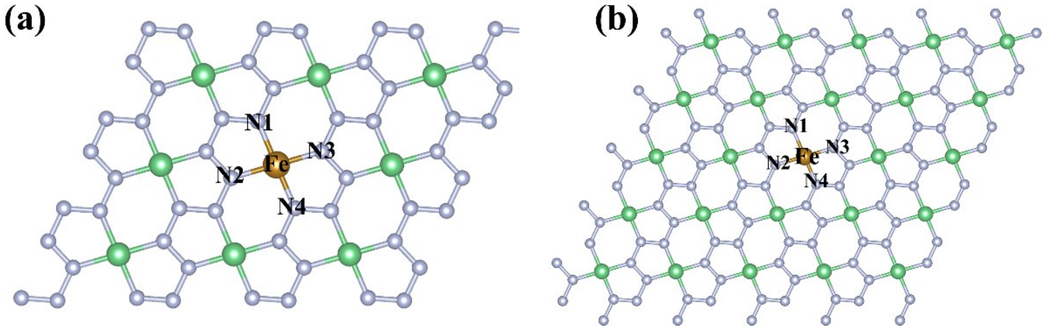

Fig. S11 *(a)3×3×1(b)5×5×1 Fe@BeN$_4$ monolayer supercells. The green, yellow and gray spheres represent Be, Fe, N atoms, respectively.*

To better understand the kinetics of TM@BeN_4 system, we calculated the free energy diagrams for TM@BeN_4 catalysts under a typical applied voltage of 2.0 V as shown in Figure S12 (a). Additionally, to clearly illustrate the trends for Fe@BeN_4 and Ir@BeN_4, we presented the driving force for each step of the reaction in Figure S12(b). The minimum energy change of Ir@BeN_4 catalyst is 0.37 V at the step from *O to *OOH, which reflects the minimum driving kinetic energy during the four-electron transfer OER process. While the minimum kinetic energy is 0.44 V during the transition from *O to *OOH in Fe@BeN_4 catalyst system, suggesting it has stronger driving force in the reaction pathway. Both catalysts demonstrate excellent performance compared to the initial BeN_4 and traditional noble metal catalysts, IrO_2 and RuO_2.

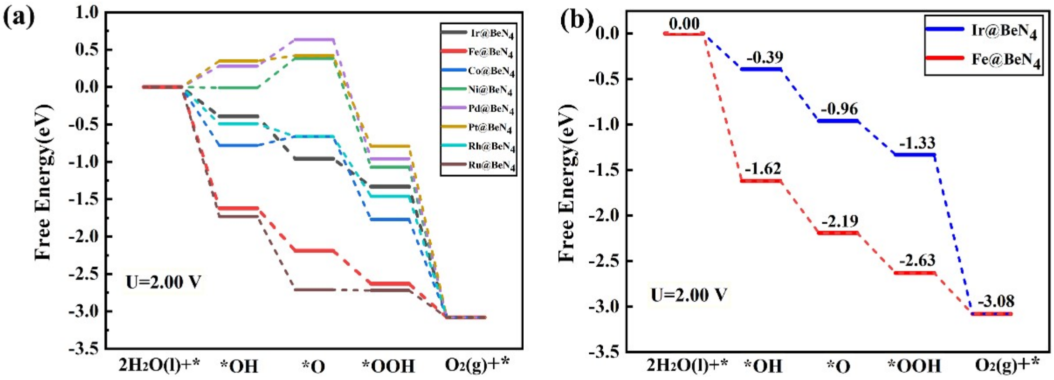

Fig. S12 *(a)The free energy step diagrams of TM@BeN_4 under an applied voltage of 2.00 V (b) Detailed free energy profiles for Fe@BeN_4 and Ir@BeN_4 under an applied voltage of 2.00 V.*

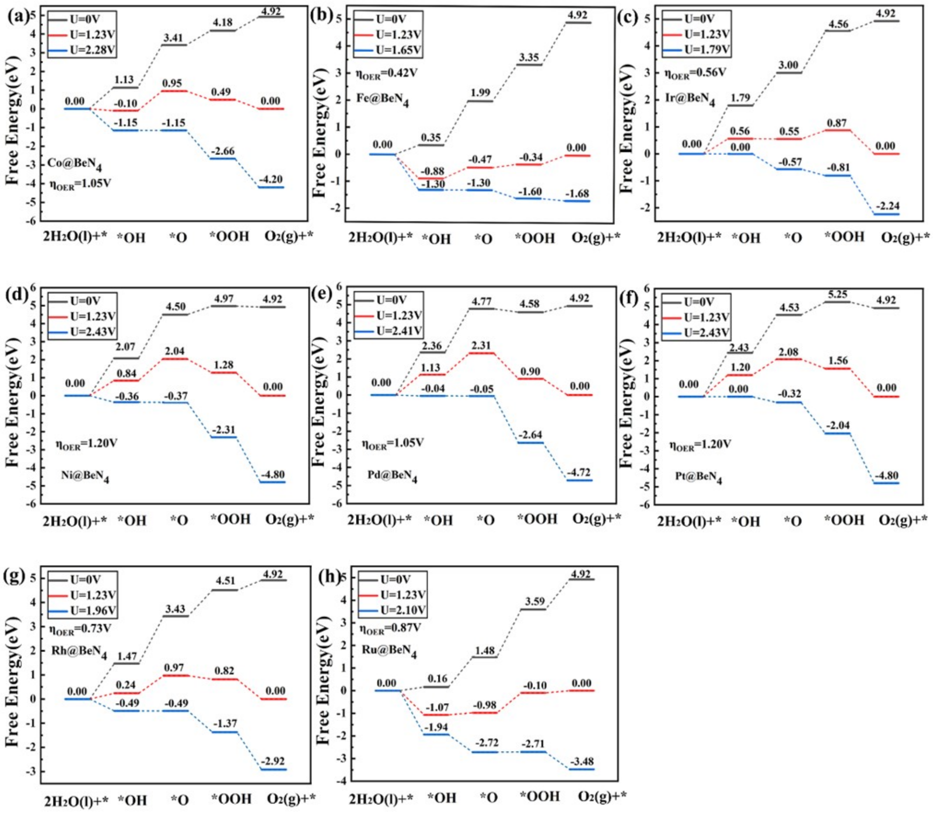

Fig. S13 *(a-h) Gibbs free energy step diagrams for OER at pH = 0 for TM@BeN_4 (TM = Fe, Co,* *Ni, Ru, Rh, Pd, Ir, Pt) by DFT + U calculations.*

To better understand the four proton-electron transfer steps in oxygen evolution reaction (OER) process, we illustrate the overpotential diagram of Fe@BeN$_4$ with reactants and products in Fig. S14, which involves four proton-electron transfer steps and we have highlighted the products of each step in blue in the diagram.

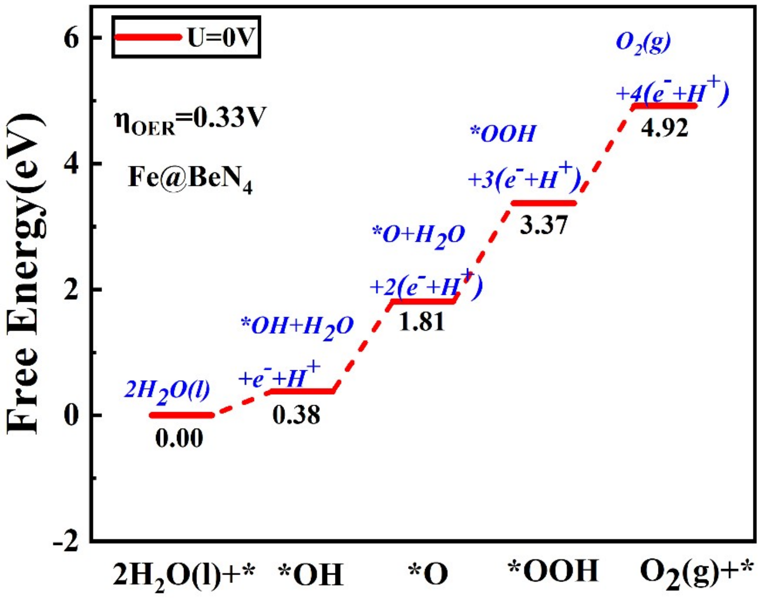

Fig. S14 *Gibbs free energy step diagrams for OER under 0V for Fe@BeN$_4$ by DFT calculations.*

To quantify the M─O bond strength, the integral of COHP (ICOHP) was performed, which reflects the electron orbital overlap degree between the metal sites and bonded O. Typically, for bonding (ICOHP < 0) and antibonding (ICOHP> 0), larger negative ICOHP values (greater absolute values) indicate stronger bonding between two atoms.

Table S2

The corresponding ICOHP values of TM-O bonding interactions of O* adsorbed on TM@BeN$_4$ TM atom

*O	Fe	Co	Ni	Ru	Rh	Pd	Ir	Pt
ICOHP	-5.04	-3.64	-2.39	-6.58	-4.33	-2.33	-4.69	-2.88

In addition, we also calculated the d-band center values and ηOER of TM@BeN$_4$ by DFT+U method (Table S3, Table S6). In the DFT+U calculations, Fe@BeN$_4$ still exhibits the largest d-band center value (-0.72 eV) and the lowest overpotential (ηOER = 0.42 V), consistent with the DFT results. Thus, we can confirm that Fe@BeN$_4$ exhibits a lower OER overpotential (ηOER = 0.33 V) in the water splitting process.

Table S3

The d-band center of TM@BeN$_4$ TM = (Fe, Co, Ni, Ru, Rh, Pd, Ir, Pt)

TM	Fe	Co	Ni	Ru	Rh	Pd	Ir	Pt
DFT-ε_d(eV)	0.10	-0.75	-2.49	-0.17	-1.00	-3.18	-0.76	-2.69
DFT+U-ε_d(eV)	-0.72	-1.52	-3.55	-1.82	-2.16	-4.88	-3.51	-4.79

Table S4

Bader charge of the *O adsorption intermediate on X-Fe@BeN$_4$

Charge Transfer	B	C	P	S	O
Fe (e)	-1.03	-1.26	-1.19	-1.28	-1.41
*O (e)	+0.64	+0.65	+0.71	+0.78	+0.72

We compared the Bader charges of atoms between the 3×3×1 and 5×5×1 Fe@BeN$_4$ monolayer supercells as shown in Fig. S11, focusing on the substituted Fe atom and its four neighboring N atoms. The detailed charge values are listed in the table S5. Our calculations show that the charge differences for corresponding atoms in both supercells range from 0.01 to 0.02e, which is within a tolerable error margin. The results indicate that the interaction between the mirror images can be ignored in the supercell.

Table S5

Bader charge of the Fe atom and its four neighboring N atoms of Fe@BeN$_4$

Bader charge	Fe	N1	N2	N3	N4
3×3×1	6.92e	5.26e	5.24e	5.24e	5.26e
5×5×1	6.90e	5.24e	5.23e	5.26e	5.25e

Table S6

The ηOER of TM@BeN$_4$ TM = (Fe, Co, Ni, Ru, Rh, Pd, Ir, Pt)

TM	Fe	Co	Ni	Ru	Rh	Pd	Ir	Pt
DFT-η(V)	0.33	0.89	1.16	0.76	0.60	1.13	0.40	1.12
DFT+U-η(V)	0.42	1.05	1.20	0.87	0.73	1.18	0.56	1.20